THE *HUBBLE SPACE TELESCOPE* KEY PROJECT ON THE EXTRAGALACTIC DISTANCE SCALE. XXVIII. COMBINING THE CONSTRAINTS ON THE HUBBLE CONSTANT[1]

JEREMY R. MOULD,[2] JOHN P. HUCHRA,[3] WENDY L. FREEDMAN,[4] ROBERT C. KENNICUTT, JR.,[5] LAURA FERRARESE,[6]
HOLLAND C. FORD,[7] BRAD K. GIBSON,[8] JOHN A. GRAHAM,[9] SHAUN M. G. HUGHES,[10] GARTH D. ILLINGWORTH,[11]
DANIEL D. KELSON,[9] LUCAS M. MACRI,[3] BARRY F. MADORE,[12] SHOKO SAKAI,[13] KIM M. SEBO,[2]
NANCY A. SILBERMANN,[12] AND PETER B. STETSON[14]

ABSTRACT

Since the launch of *Hubble Space Telescope* (*HST*) 9 yr ago, Cepheid distances to 25 galaxies have been determined for the purpose of calibrating secondary distance indicators. Eighteen of these have been measured by the *HST* Key Project team, six by the Supernova Calibration Project, and one independently by Tanvir. Collectively, this work sets out an array of survey markers over the region within 25 Mpc of the Milky Way. A variety of secondary distance indicators can now be calibrated, and the accompanying four papers employ the full set of 25 galaxies to consider the Tully-Fisher relation, the fundamental plane of elliptical galaxies, Type Ia supernovae, and surface brightness fluctuations. When calibrated with Cepheid distances, each of these methods yields a measurement of the Hubble constant and a corresponding measurement uncertainty. We combine these measurements in this paper, together with a model of the velocity field, to yield the best available estimate of the value of H_0 within the range of these secondary distance indicators and its uncertainty. The uncertainty in the result is modeled in an extensive simulation we call the "virtual Key Project." The velocity-field model includes the influence of the Virgo cluster, the Great Attractor, and the Shapley supercluster, but does not play a significant part in determining the result. The result is $H_0 = 71 \pm 6$ km s^{-1} Mpc^{-1}. The largest contributor to the uncertainty of this 67% confidence level result is the distance of the Large Magellanic Cloud, which has been assumed to be 50 ± 3 kpc. This takes up the first 6.5% of our 9% error budget. Other contributors are the photometric calibration of the WFPC2 instrument, which takes up 4.5%, deviations from uniform Hubble flow in the volume sampled ($\lesssim 2\%$), the composition sensitivity of the Cepheid period-luminosity relation (4%), and departures from a universal reddening law ($\sim 1\%$). These are the major components that , when combined in quadrature, make up the 9% total uncertainty. If the LMC distance modulus were systematically smaller by 1 σ than that adopted here, the derived value of the Hubble constant would increase by 4 km s^{-1} Mpc^{-1}. Most of the significant systematic errors are capable of amelioration in future work. These include the uncertainty in the photometric calibration of WFPC2, the LMC distance, and the reddening correction. A NICMOS study is in its preliminary reduction phase, addressing the last of these concerns. Various empirical analyses have suggested that Cepheid distance moduli are affected by metallicity differences. If we adopted the composition sensitivity obtained in the Key Project's study of M101, and employed the oxygen abundances measured spectroscopically in each of the Cepheid fields we have studied, the value of the Hubble constant would be reduced by 4% $\pm$ 2% to 68 ± 6 km s^{-1} Mpc^{-1}.

Subject headings: Cepheids — cosmology: observations — distance scale — galaxies: distances and redshifts

1. INTRODUCTION

The goal of the *Hubble Space Telescope* (*HST*) Key Project on the Extragalactic Distance Scale was announced in 1984 by the newly formed Space Telescope Science Institute: the determination of the Hubble constant to an accuracy of $\lesssim 10\%$. The recommended approach was classical, to use Cepheid distances to calibrate secondary distance indicators. A plan was developed (Aaronson & Mould 1986), and our proposal was selected, but the project did not get into top gear until *HST*'s spherical aberration had been corrected. This observing program, which is now complete, has been described in detail by Kennicutt, Freedman, & Mould (1995).

The accompanying four papers (Sakai et al. 2000; Gibson et al. 2000; Kelson et al. 2000; Ferrarese et al. 2000a) show how Cepheid distances to 18 spirals within ~ 25 Mpc are used to calibrate the Tully-Fisher relation for spiral galaxies (TF), the fundamental plane for elliptical galaxies (FP), surface brightness fluctuations (SBF), and (with the six additional galaxies of the supernova calibration project) Type Ia supernovae (SNe Ia). Each of these distance indicators is able to penetrate to sufficient distance (10^4 km s^{-1}) that perturbations in the Hubble flow are small compared to the expansion of the universe. None of them is free from implicit assumptions about the stellar population of the galaxies whose distances are being measured. That is the case whether we assume constancy of the mass-to-light ratio between the galaxies whose Cepheid distances we have measured ("the calibrators") and galaxies in, say, the Coma cluster, or whether we assume that supernova progenitors are essentially similar in the calibrators and the Calán/Tololo survey galaxies. It therefore seems more prudent to combine constraints from four separate secondary distance indicators with different systematics than to investigate one alone.

The purpose of the present paper is to show how these constraints on H_0 can be combined to yield the local Hubble constant to an accuracy of $\lesssim 10\%$ at the 1 σ confidence level. In a subsequent paper (W. Freedman et al., in preparation) we examine the extrapolation to a sufficiently larger volume as a step from a local value of H_0 to the global expansion rate.

2. THE KEY PROJECT DISTANCE DATABASE AND VELOCITY FIELD MODEL

The primary product of the Key Project has been the discovery of Cepheids in a set of galaxies within 25 Mpc and the measurement of their characteristics. The galaxy distances inferred by means of period-luminosity (PL) relations are collected by Ferrarese et al. (2000b). Secondary distance indicators extend the range of measurement into the redshift range 2000–10,000 km s^{-1}, and it is then necessary to relate the recession velocities of these objects to the smooth Hubble flow.

One of the major remaining uncertainties in the determination of the Hubble constant is the correction of the observed velocities of our tracers for large-scale motions. Twenty years ago, the "cosmic" velocities of objects were simply taken to be their velocities corrected for Galactic rotation and sometimes additionally corrected to the centroid of the Local Group. Slightly more than 20 yr ago, the apparent motion of the Milky Way and, by inference,

the Local Group with respect to the cosmic microwave background (CMB) was discovered, and it has now been exquisitely measured with *COBE* (Kogut et al. 1993). Slightly less than 20 yr ago, the infall of the Local Group into the core of the Local Supercluster that had been predicted by de Vaucouleurs (1958, 1972), Peebles (1976), Silk (1974), and others was detected (Tonry & Davis 1981; Davis et al. 1980; Aaronson et al. 1982, 1980). Soon after, larger scale flows were seen (Burstein et al. 1986; Lynden-Bell et al. 1988).

It is now clear (e.g., Strauss & Willick 1995) that there are motions on scales of tens of Mpc with amplitudes up to the order of the Milky Way's motion with respect to the CMB. However, the exact nature of these motions with respect to the CMB is still unclear (Lauer & Postman 1994; Riess, Press, & Kirshner 1995), as are the precise causes of our motion.

Recently, several groups have chosen to treat this problem by correcting apparent velocities to the CMB frame. This is generally done by simply applying a correction that is our CMB velocity (~ 630 km s^{-1}) times the cosine of the angle between the direction of motion with respect to the CMB. At large velocities, $cz \geq 10,000$ km s^{-1}, unless there are peculiar velocities on much larger scales or with much larger amplitudes than hitherto seen, this correction is both small and probably proper. Not correcting for it, in fact, can introduce a bias in the determination of H_0 that could be as large as $V_{\rm CMB}/V_{\rm object}$, or 6%. In fact, for any sample of objects not uniformly distributed with respect to $\cos \theta_{\rm CMB}$, such bias could be a nonnegligible contribution to the error in H_0.

Worse than that, at smaller redshifts, the flow field is much more complicated (e.g., Dekel et al. 1999); near the centers of rich clusters, the infall amplitudes and/or the velocity dispersion can be very large ($\gtrsim 1000$ km s^{-1}), and for nearby objects peculiar motions can be a substantial part of the observed velocity. It is also clear that it is a mistake to correct the velocities of very nearby objects by a simple $\cos \theta_{\rm CMB}$ term, because nearby objects (e.g., M31 or the M81 group) are closer to being at rest with respect to the Local Group frame than with respect to the CMB frame.

To treat this problem for our various determinations of H_0 via several different samples of groups, clusters, and individual galaxies, we have developed a simple linear multiattractor model based on the Han & Mould (1990) and Han (1992) models, similar to the multiattractor model advocated by Marinoni et al. (1998a). The model is linear and assumes (1) a flow toward each attractor (e.g., Virgo, the Great Attractor) that is independent of each object, so that the corrections for each are additive; (2) flows described by a fiducial infall velocity at the position of the Local Group toward each attractor (see Peebles 1976; Schechter 1980); and (3) an essentially cylindrical (section of a cone) masked volume around each attractor where objects are forced to the attractor's velocity. This last procedure collapses the cluster cores and avoids our having to deal with regions where the flow field is certainly nonlinear and usually multivalued for any observed velocity. We add one additional simplifying assumption, (4) that to first order, peculiar velocities are small enough that an object's apparent velocity in the Local Group frame is the estimate of its distance. Again, this assumption is generally justified for objects far from our attractors. With these assumptions, it is

trivial to include additional attractors (e.g., the Shapley Supercluster; Scaramella et al. 1989) if desired.

The simple linear infall model has been described by a number of authors, most notably Schechter (1980). In this model, the estimated radial component (with respect to the Local Group) of peculiar velocity induced by an attractor is, by the law of cosines,

$$V_{\rm infall} \approx V_{\rm fid} \cos \theta + V_{\rm fid} \left(\frac{V_o - V_a \cos \theta}{r_{oa}} \right) \left(\frac{r_{oa}}{V_a} \right)^{1-\gamma} , \quad (1)$$

where $V_{\rm fid}$ is the amplitude of the infall pattern to that attractor *at the Local group*, V_o is the observed velocity of the object (in the LG frame), V_a is the observed distance of the attractor expressed as a velocity, γ is the slope of the attractor's density profile, $\rho(r) \propto r^{-\gamma}$, θ is the projected angle between the object and the attractor, and r_{oa} is the estimated distance of the object from the attractor expressed as a velocity,

$$r_{oa} = \sqrt{V_o^2 + V_a^2 - 2V_o V_a \cos \theta} . \quad (2)$$

The first term in equation (1) is the projection of the LG infall velocity into the attractor ($V_{\rm fid}$), and the second term is the projection of the object's infall into the attractor.

Note that we have modified the normal form of this relation, which uses the true relative distances of the objects in question, to instead express distances as velocities. To produce our simple flow-field corrections, rather than solve for the actual relative distances of the objects in question, we have assumed that, to first order, the apparent radial velocity of an object (in the Local Group frame) represents its distance. We fix and use the cosmic velocity of the attractors, after solving for their own motions with respect to the other attractors. A more complete treatment would iteratively solve for the true velocity of each source, and an even more complete treatment would be to use the actual observed density field (Marioni et al. 1998b), but since our goal is to provide just a first-order flow-field correction to investigate and eliminate significant flow-field biases in our H_0 determinations, we stop here. The details are given in Appendix A.

This seems reasonable, given the uncertainty in the absolute distance and location for the main attractors, our significant lack of knowledge of the flow field at distances much beyond 4500 km s^{-1}, and the other simplifying assumptions that are generally made, such as assuming spherical attractors. We will test the above assumption in future work (J. P. Huchra, in preparation), and implement an iterative solution to the flow-field corrections if it is warranted. For the present, we note that if we abandon our flow-field model and assume instead that only the observer is in motion relative to the smooth Hubble flow, the maximum change in our result for H_0 would be a 4% increase in the SBF result. There would be a 2% decrease in the result from supernovae, and smaller effects from TF and FP.

3. THE VIRTUAL KEY PROJECT

The cosmic distance ladder is a notable example of the concatenation of measurement uncertainties in a multistep experiment (Rowan-Robinson 1986). Careful distinction between random and systematic error is required (e.g., Madore et al. 1998), and bias is a concern (Sandage 1996).

For the purposes of this paper, we have developed a simulation code that recreates the Key Project in the computer, allowing the uncertainties and parameter dependences to be followed extensively and investigated rigorously.

One fundamental assumption of the Key Project is that the distance of the Large Magellanic Cloud is 50 kpc ($m - M = 18.50 \pm 0.13$ mag). Indeed, our result might best be expressed in units of km s^{-1} per LMC distance. Nevertheless, a 6.5% uncertainty in the distance of the LMC is incorporated in the project error budget. In § 5, we also explore the use of a literature survey (Fig. 1) as a probability distribution function for the LMC distance. Westerlund's (1996) survey has been updated, as discussed in more detail by W. Freedman et al. (in preparation).

The LMC Cepheid PL relation in the simulation also has a 0.02 mag zero-point uncertainty (Madore & Freedman 1991; Tanvir 1999). This estimate will be tested when photometry of a larger sample of LMC Cepheids is complete (K. Sebo et al., in preparation). A second systematic error in the Key Project arises from the residual uncertainty of WFPC2's correction for charge transfer efficiency (see Appendix B) and calibration on to the (V, I) system. This is amplified to a 0.09 mag uncertainty in distance modulus by
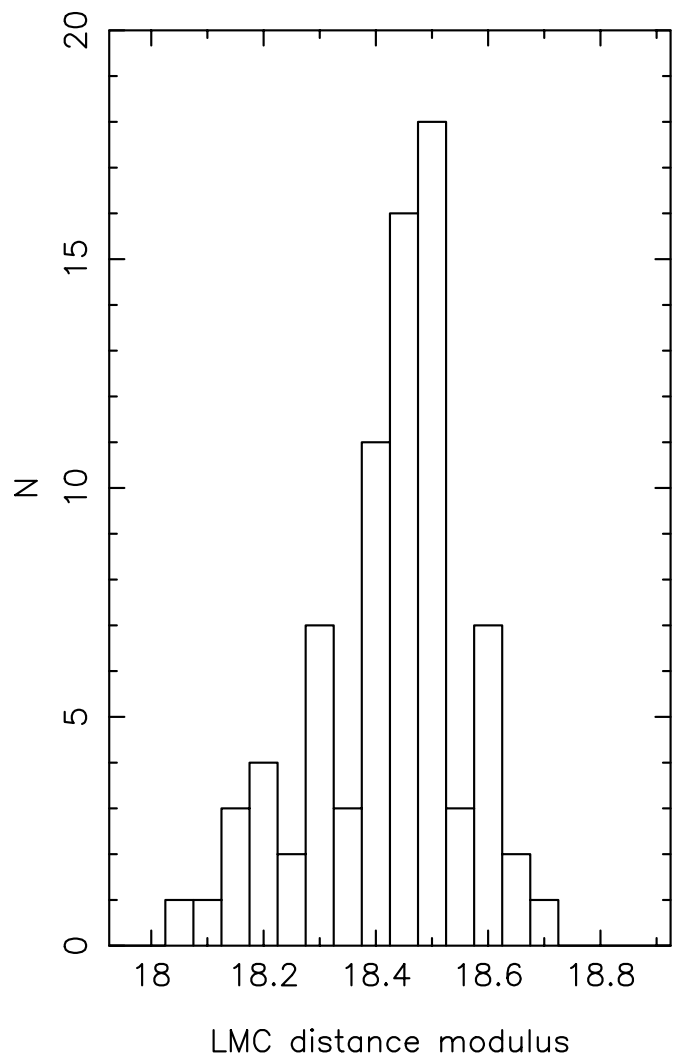

FIG. 1.—Distribution of published LMC distance moduli from the literature. Values from 1983–1995 are from the review by Westerlund (1996). Values up to the end of 1998 have been collated by Freedman (1999).
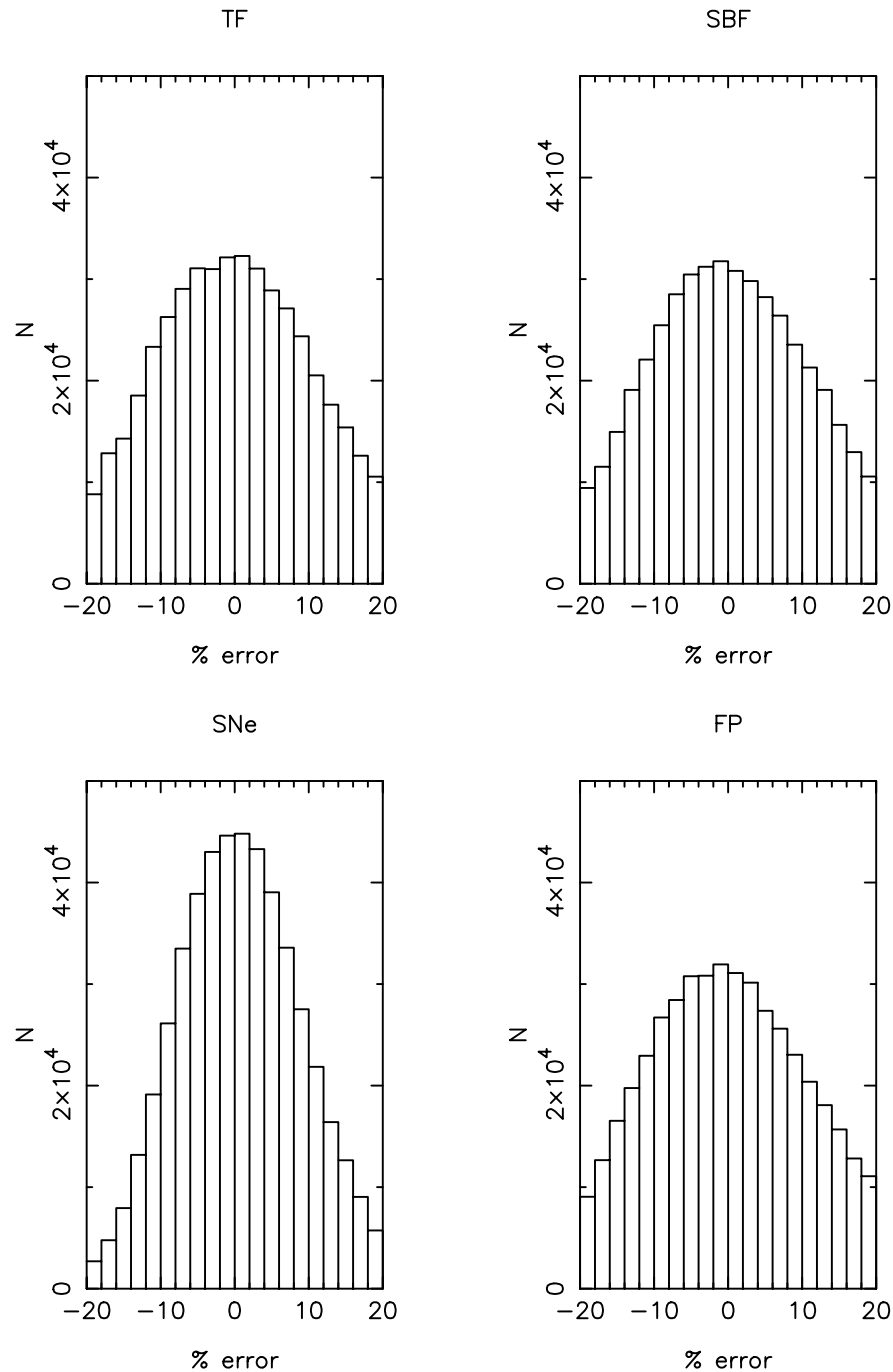
FIG. 2.—Distribution of uncertainties in H_0 for each of the four secondary distance indicators calibrated and applied in the virtual Key Project

the approach we have adopted to reddening correction, because each galaxy's absolute distance modulus is a linear combination of the apparent moduli, $\mu_0 = 2.45\mu_I - 1.45\mu_V$.

The metallicity dependence of the PL relation has proved difficult to constrain (Kennicutt et al. 1998). For most of the galaxies for which we have measured Cepheid distances, however, measurements of oxygen abundances in H II regions in or near the Cepheid fields are also available. Sakai et al. (2000), Gibson et al. (2000), Kelson et al. (2000), and Ferrarese et al. (2000a) present results, both neglecting PL-Z and correcting the galaxy distances published in Papers I–XXI by the coefficient $\gamma_{VI} = d(m - M)/d[\text{O/H}] = -0.24 \pm 0.16$ mag dex^{-1} (Kennicutt et al. 1998), and this is followed in the simulation. In each simulation a value of γ is

drawn from a normal distribution for this purpose. Normal distributions are employed throughout these simulations, except where otherwise noted.

For each of the galaxies in the virtual Key Project, a Cepheid distance is generated assuming a 0.05 mag intercept uncertainty in its PL-V relation and a similar intercept uncertainty in PL-I. These are typical values; some of the real galaxies have more Cepheids and better-determined distances (e.g., NGC 925), and others have fewer Cepheids (e.g., NGC 4414), and hence larger uncertainties. Implicitly, we have assumed that the reddening law is universal, adopting an uncertainty in its slope of $R_V = 3.3 \pm 0.3$. As a follow-up to the Key Project, this will be tested with NICMOS observations of *HST* Cepheids for some galaxies.
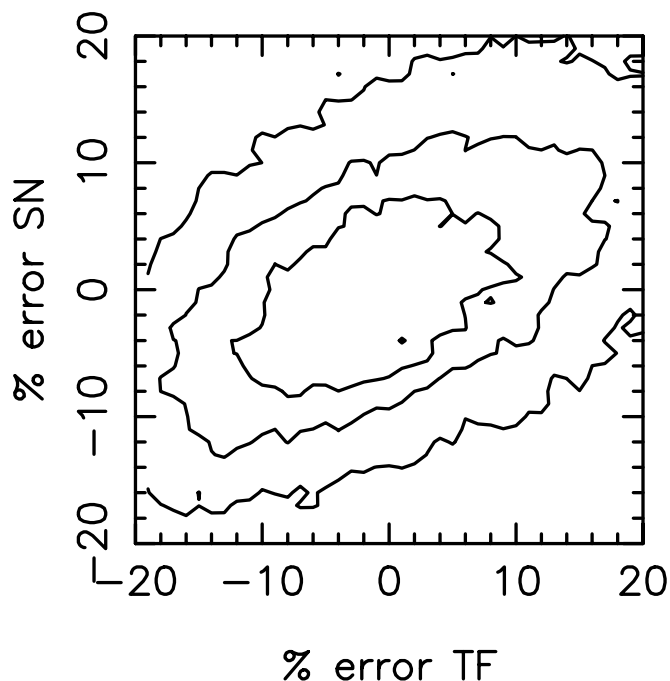
FIG. 3.—Percentage error contours for the supernova and Tully-Fisher measurements of H_0. The outer contour encloses 80% of the realizations.

A primary, and long awaited (Aaronson & Mould 1986), outcome of the Key Project is a calibration of the TF relation. Sakai et al. (2000) find an rms scatter about this relation, and this is included in the 18 galaxy calibration simulation. The calibration is then applied to a sample of five clusters with $cz > 5000$ km s^{-1} (and this is then all realized half a million times.) Sakai et al. analyze a larger sample than this, but their final result is based on the most distant members of the cluster data set. Comparison of the simulated and input Hubble relations yields an H_0 error from the TF calibration component of the Key Project.

In the simulation, velocities are drawn from a normal distribution with $\sigma = 300$ km s^{-1} (Giovanelli et al. 1998). The real flow field is more complex, and the model adopted by Sakai et al. (2000), Gibson et al. (2000), Kelson et al. (2000), and Ferrarese et al. (2000a) is specified in Appendix A. We have incorporated the Tully-Fisher error budget given by Sakai et al. in their Table 6. Noting the discrepancy they report between cluster distances based on I-band photometry and those based on H-band photometry, we adopt an uncertainty of 0.18 mag to allow for systematics in the galaxy photometry.

Second, the Key Project provides a very direct calibration of the SBF relation. Following Ferrarese et al. (2000a), the simulation takes six galaxies and derives a zero point for the relation between SBF magnitude and color. This relation, which is assumed to have an rms scatter of 0.11 mag (Tonry et al. 1997), is then applied to the four galaxies in the redshift range 3000–5000 km s^{-1} with HST Planetary Camera SBF measurements. We have omitted Coma and NGC 4373, just as Ferrarese did. Comparison of the simulated and input Hubble relations yields an H_0 error from the SBF calibration component of the Key Project. The approach here follows the error budget given in Table 5 of Ferrarese et al. (2000a).

The third, and in some respects strongest, component of the distance scale calibrated by HST's Cepheid database is the relation between the maximum luminosity of the SN Ia light curve and the supernova decline rate (Hamuy et al. 1996; Phillips et al. 1999). Uncertainties in the observed magnitudes and reddening of the supernovae and their Cepheid distances affect the calibration. In the simulation, we have adopted the uncertainties quoted by Gibson et al. (2000) for six calibrators and incorporated the error budget given in their Table 7. The calibration was then applied to the 27 supernovae of Hamuy et al. between 6000 and 30,000 km s^{-1}.

Finally, to simulate the calibration of the fundamental plane, we have employed the error budget in Table 3 of Kelson et al. (2000) and assumed that the Leo ellipticals lie within 1 Mpc of the respective mean distances of their Cepheid-bearing associates. In the case of Virgo and Fornax, we have assumed the elongation of the cluster along the line of sight described by Gonzales & Faber (1997) as an exponential falloff with a 2.5–4 Mpc scale length. The calibration is then applied to eight clusters, ranging from Hydra to Abell 3381 in distance. We have assumed that the clusters have the same 300 km s^{-1} rms noise that is seen in the TF sample.

4. THE ERROR DISTRIBUTIONS

Based on 5×10^5 realizations, Figure 2a shows that the simulated TF error distribution, which gives the probability that the H_0 determined by Sakai et al. (2000) alone has a given percentage error, is rather normal looking, biased at no more than the 1% level, and has $\sigma_{TF} \approx 12\%$. In fact, Sakai et al. have produced four realizations of the TF H_0 measurement at different wavelengths, obtaining 74 km s^{-1} Mpc^{-1} from an I-band calibration and 67 km s^{-1} Mpc^{-1} from an H-band calibration. The chance that this 10% discrepancy would occur by chance, especially when the same calibrator distances have been assumed in both cases, is small. Sakai et al. consider systematics in the line widths, I-band extinction corrections, and H-band aperture/diameter ratios as possible contributors to this discrepancy. Uncertain homogeneity in galaxy diameters leads to lower weight for the H-band result.

The other panels in Figure 2 show the SBF error distribution, the SN error distribution, and the FP error distribution. The narrowest is the SN error distribution (9% rms, compared with 12% in the other two cases). Figure 3 shows the covariance between the SN and TF calibration errors, which occurs because a number of the SN Ia calibrators are also TF calibrators. Cepheid-bearing galaxies represent only a selected sample (or, in the FP case, merely neighbors) of the population of galaxies to which the calibration we have derived is applied. Stellar population effects are calibrated empirically in the case of SBF, but we make no allowance for parameters (beyond decline rate and reddening), which may still remain hidden in the SN case.

5. COMBINING THE CONSTRAINTS

The results of the previous section will aid us in optimally combining the four secondary distance indicators. We can compare $\langle H_0 \rangle$ from a straight mean of the four measurements and compare this with a weighted mean. We choose weights for H_0^{TF} and H_0^{SBF} that are the inverse of σ_{TF}^2 and σ_{SBF}^2, respectively. Effectively, this 1.5 times weights the SN distance indicator relative to the other three.

Combining $H_0^{\mathrm{TF}} = 71 \pm 4$ (random) ± 7 (systematic) (Sakai et al. 2000) with $H_0^{\mathrm{SBF}} = 69 \pm 4 \pm 6$ (Ferrarese et al. 2000a), $H_0^{\mathrm{FP}} = 78 \pm 8 \pm 10$ (Kelson et al. 2000), and $H_0^{\mathrm{SNIa}} = 68 \pm 2 \pm 5$ (Gibson et al. 2000), we obtain $H_0 = 71 \pm 6$ km s^{-1} Mpc^{-1}, without the weighting influencing the outcome a great deal. The error distribution for the combined constraints is shown in Figure 4. The width of this distribution is $\pm 9\%$ (1 σ).

A dimension that each of the error distributions shares is dependence on the assumed distance of the LMC. This is illustrated in Figure 5, which shows 67% probability contours for each of the four secondary distance indicators. The only comparable distance indicator in the local volume that does not depend on the LMC distance (but is still influenced by SN 1987A) is the expanding photospheres method applied to supernovae of Type II. This yields $H_0 = 73 \pm 12$ km s^{-1} Mpc^{-1} (Schmidt et al. 1994) at 95% confidence.

If we adopt Figure 1 as the probability distribution of the distance of the LMC, the error distributions broaden and reflect the skew seen in Figure 1. The combined constraint is shown in Figure 6. The uncertainty in H_0 grows to 12% and the bias, the amount by which H_0 is underestimated through our assumption of a 50 kpc distance, becomes 4.5%. It is likely that Figure 1 exaggerates the probability of LMC distance moduli as low as 18.1 mag, since it weights recent estimates based on the brightness of the "red clump" almost as highly as it weights Cepheids. A review of the literature on the LMC distance is provided by W. Freedman et al. (in preparation). Expressing our result as a self-contained experiment, we obtain $H_0 = 3.5 \pm 0.2$ km s^{-1} per LMC distance.

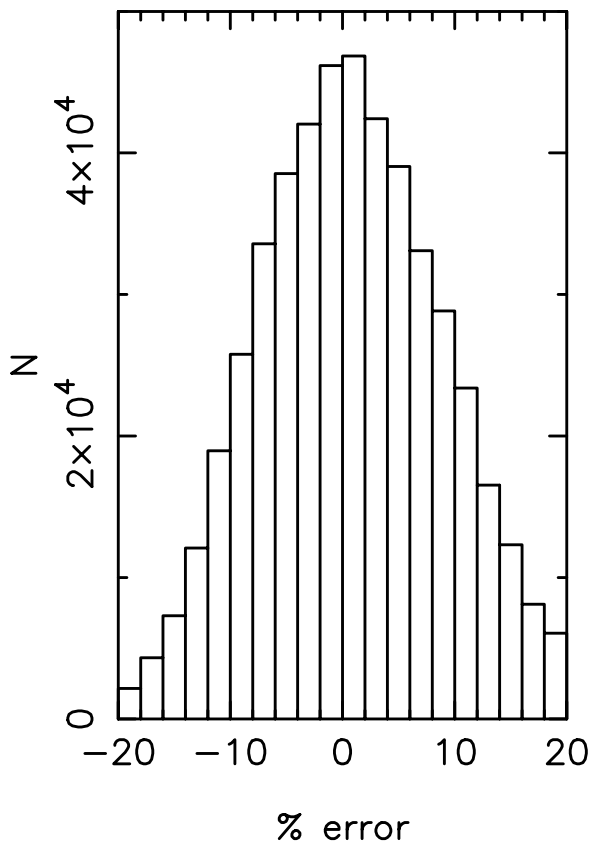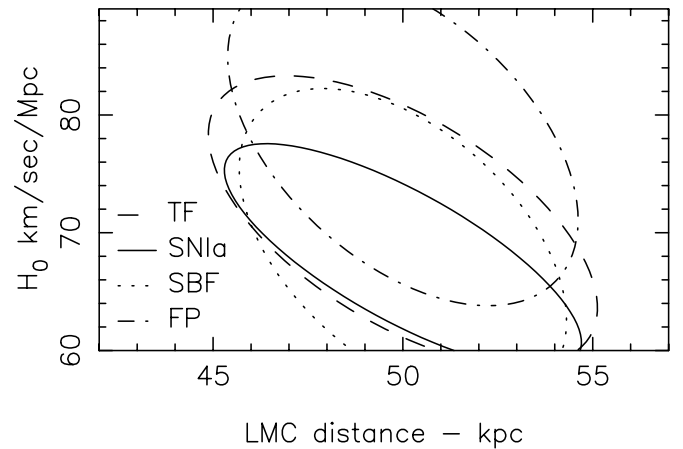Fig. 5.—Key Project calibration constrains H_0 in four ways, but these are each, in turn, dependent on the assumed distance of the LMC, which provides the reference Cepheid PL relation for the project.

We conclude that the expansion rate within the area mapped by the secondary distance indicators we have calibrated is 71 ± 6 km s^{-1} Mpc^{-1}. The distribution of galaxies in Figure 7 renders this result relatively immune to a low-amplitude bulk flow of the sort detected by Giovanelli

Fig. 4.—Uncertainty distribution for the combined constraints on H_0
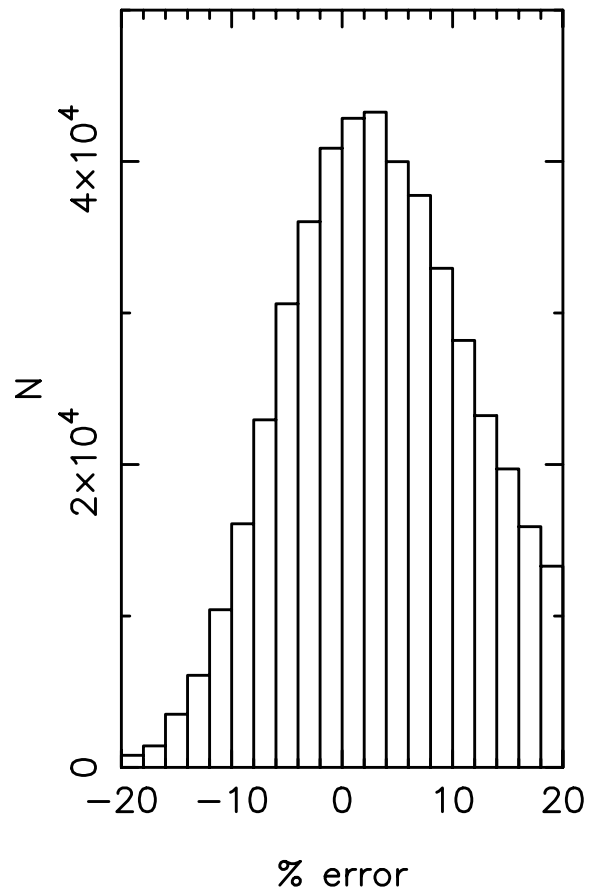

Fig. 6.—Corresponding distribution calculated from the probability distribution of LMC distances in Fig. 1.
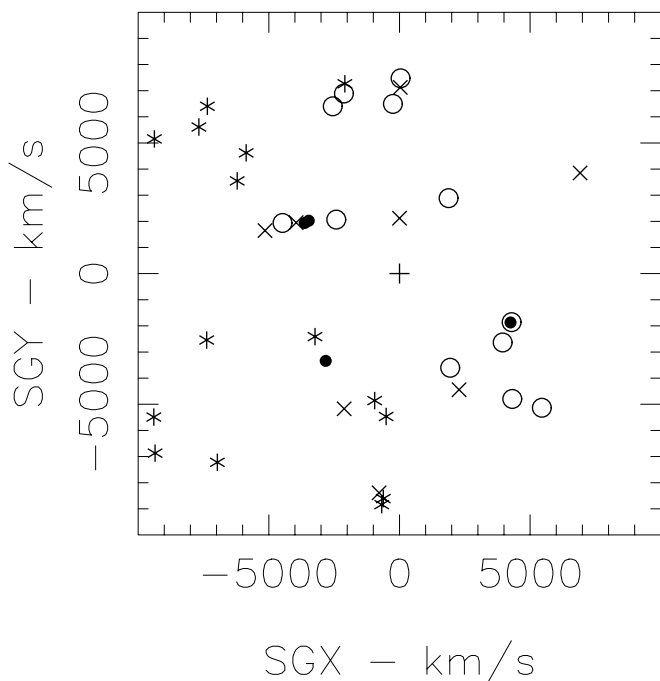
FIG. 7.—Distribution of secondary distance indicators in projection on the supergalactic plane. *Open circles*, TF clusters from Sakai et al. (2000); *solid circles*, SBF clusters from Ferrarese et al. (2000a); *asterisks*, SNe Ia from Hamuy et al. (1996); *crosses*, FP clusters from Kelson et al. (2000).

et al. (1998). Similarly, velocity perturbations due to a Com-acentric bubble or a Local Void (Tully & Fisher 1987) would tend to generate a dipole in Giovanelli's results, which is not seen, at least in the Arecibo sky sample available to date.

Finally, we note that adoption of the metallicity dependence of the Cepheid PL relation described in § 3 reduces the combined H_0 by 4%, to 68 ± 6 km s^{-1} Mpc^{-1}.

6. FUTURE WORK

A large-scale, locally centered bubble would require that this local H_0 be corrected for the density anomaly.

Tammann (1998) and Zehavi et al. (1998) have estimated that this amounts to a few percent, and this deserves careful evaluation, focused on the volume sampled in the accompanying papers. Truly *large*-scale density perturbations are correspondingly unlikely (Shi & Turner 1998).

To complete the Key Project, we intend to examine this matter and several other limitations of current work that have been identified here and in the accompanying papers. These include the limited LMC Cepheid PL relation, the excessively large uncertainty in the photometric calibration we have adopted for WFPC2, and the comparison of results from this classical approach to the extragalactic distance scale with recent progress in the analysis of gravitationally lensed quasar time delays and the X-ray gas in rich clusters of galaxies (the Sunyaev-Zeldovich effect). This work is in progress (W. Freedman et al., in preparation). The Key Project's error analysis will also be developed in more detail than we have presented here.

These additional steps should secure the Key Project's goal, a 10% Hubble constant, to a higher level of confidence than the 1 σ level reported here.

APPENDIX A

THE LOCAL FLOW FIELD

The model outlined in § 2 employs a five-step procedure to convert heliocentric velocities to velocities characteristic of the expansion of the universe.

1. Correction of the observed heliocentric velocity of our objects to the centroid of the Local Group. Here we use the Yahil, Tammann, & Sandage (1977) prescription (YST) for consistency, but note that use of other prescriptions (e.g., the IAU 300 sin *l* cos *b*) generally does not make a large difference beyond halfway to Virgo. The YST correction to the Local Group centroid is

$$V_{\rm LG} = V_H - 79 \cos l \cos b + 296 \sin l \cos b - 36 \sin b . \tag{A1}$$

As indicated in § 2, we set $V_0 = V_{\rm LG}$.

2. Correction for Virgo infall. Note that the Virgo cosmic velocity is derived by correcting the observed heliocentric velocity[15] to the LG centroid for our infall velocity and for its infall into the GA. Note also that the correction for Virgo infall

---

[15] See Huchra (1995), at the Heron Island Proceedings, http://www.mso.anu.edu.au/~heron/Huchra/huchra.html.

TABLE A1

MODEL PARAMETERS

Cluster	R.A. (1950)	Decl. (1950)	V_H[a] (km s^{-1})	V_{LG}[b] (km s^{-1})	V_{fid}[c] (km s^{-1})	Radius[d] (deg)	V_{range}[e] (km s^{-1})
Virgo	12 28 19	+12 40	1035	957	200	10	600–2300
GA	13 20 0	44 00	4600	4380	400	10	2600–6600
Shapley	13 30 0	31 00	13800	13600	85	12	10,000–16,000

NOTE.—Units of right ascension are hours, minutes, and seconds, and units of declination are degrees and arcminutes.

[a] Observed (mean) heliocentric velocity.

[b] Velocity corrected to the centroid of the Local Group using the $300 \sin l \cos b$ prescription.

[c] Adopted model infall velocity at the position of the LG.

[d] Assumed cluster radius in degrees.

[e] Velocity range collapsed for the cluster core (heliocentric). The radius and range give the partial cone that is zeroed to the attractor center in the flow-field program.

includes *two* components, the change in velocity due to the infall of the object into Virgo plus the vector contribution due to the Local Group's peculiar velocity into Virgo. That term is just $V_{fid} \cos (\theta_v)$.

3. Correction for GA infall as in point 2.

4. Correction for Shapley supercluster infall. The correction adopted is set so that it reproduced the amplitude of the CMB dipole as $V \to \infty$.

5. Correction for other concentrations, as necessary.

Since we have set the solution to be additive, the final corrected "cosmic" velocity with respect to the LG is then

$$V_{cosmic} = V_H + V_{c,LG} - V_{in, Virgo} - V_{in, GA} - V_{in, Shap} - \cdots , \qquad (A2)$$

where V_H is the observed heliocentric velocity and $V_{c,LG}$ is the correction to the Local Group centroid described above. Note that the STY correction to the Local Group centroid is *not* the same as the IAU correction, so some of the models and assumptions made in earlier Virgo flow fits must be modified. We have used the YST assumption primarily because this is what was used to derive the corrected CMB dipole.

For our initial attempt at a detailed flow-field correction, we include just three attractors: the Local Supercluster, the Great Attractor, and the Shapley Supercluster. The parameters we use for the attractors are given in Table A1 and are taken (and estimated) from a variety of sources including AHMST, Han (1992), Faber & Burstein (1989), Shaya, Tully, & Pierce (1992), and Huchra (1995).[16] For simplicity, we also assume $\gamma = 2$. For this first-cut model, we assume an infall into Virgo of 200 km s^{-1} at the LG, an infall into the GA of 400 km s^{-1}, and an infall into Shapley of 85 km s^{-1}. These numbers give good agreement with the amplitude of the CMB dipole, but with only these three attractors, the direction of maximum LG motion is 27° away from the CMB direction.

APPENDIX B

THE PHOTOMETRIC ZERO POINT

The status and calibration of the Wide Field Planetary Camera 2 (WFPC2) has been reviewed by Gonzaga et al. (1999), who find that photometric accuracies of a few percent are routinely possible. The baseline photometric calibration for WFPC2 is given by Holtzman et al. (1995). The standard calibration for Papers IV–XXI in the Key Project series is that of Hill et al. (1998), and accounts for the principal systematic CTE effect, the so-called long vs. short exposure effect (Wiggs et al. 1999). Photometric stability has been satisfactory over the duration of the project with fluctuations of $\lesssim 2\%$ or less peak-to-peak over 4 yr at the wavelengths observed here (Heyer et al. 1999).

Images obtained with the CCDs in WFPC2 are known to be subject to charge loss during readout, presumably due to electron traps in the silicon of the detectors. Approximate corrections for this charge loss have been published by Whitmore & Heyer (1997) and Stetson (1998), but these corrections are based on comparatively short exposures of comparatively bright stars, so the observations exhibit a comparatively narrow range of apparent sky brightness. Furthermore, the zero points of the WFPC2 photometric system are primarily determined from comparatively bright stars, since those are the ones for which the ground-based photometry is most reliable. Since the amount of charge lost from a stellar image appears to be a function of both the brightness of the star image and the apparent brightness of the sky, these dependencies must be quite well determined to enable reliable extrapolation from bright stars as observed against a faint sky (standard stars in relatively uncrowded fields in short exposures) to faint stars observed against a bright sky (distant Cepheids project against galactic disks in long exposures). The study of Stetson (1998) was intended to provide that extrapolation, based on comparatively short exposures of the nearby globular cluster ω Centauri, and both short and long exposures of the remote globular cluster NGC 2419. These data seemed to yield consistent charge-loss corrections and zero points, but various tests suggested that there remained some uncontrolled systematic effects that might amount to of the order of ± 0.02 mag or so in each of the V and I filters.

---

[16] Huchra (1995) available at the Heron Island Proceedings, http://www.mso.anu.edu.au/~heron/Huchra/huchra.html.

Improved corrections for charge-transfer efficiency effects in the WFPC2 CCDs has been presented by Stetson (1998). Presumably because of different illumination levels, correction of our photometry affects the V and I magnitudes differently. In the mean, and based on the reference stars' photometry published in Papers IV–XXI, distance moduli on the Stetson (1998) system are 0.07 ± 0.02 mag closer than on the Hill et al. system.

In attempting to improve upon this situation, P. Stetson (in preparation) has added ground-based and WFPC2 data for the nearby globular cluster M92 (= NGC 6341) to the solution. The WFPC2 data for M92 are intermediate in exposure time between those for ω Cen and the short exposures of NGC 2419 on the one hand, and the long exposures of NGC 2419 on the other. As in Stetson (1998), the ω Cen, NGC 2419, and M92 data were all combined into a single solution to determine the optimum coefficients relating the amount of charge lost from a stellar image to its position on the detector, its brightness, and the surface brightness of the local sky. When these corrections are applied to determine the optimum photometric zero points from the data for each globular cluster, it is found that the results for ω Cen and NGC 2419 are consistent, as before, but the zero points implied by the M92 data are substantially different: $+0.054 \pm 0.003$ mag in V and -0.038 ± 0.003 in I. Adoption of a zero point based on M92 would move the Key Project galaxies 0.14 mag closer than the Hill et al. (1998) reference point.

On the other hand, Saha (in preparation) finds different results from analysis of cycle 7 calibration data. He has determined that CTE correction will yield Cepheid colors bluer by ≈ 0.02 mag, corresponding to distance moduli *more distant* by 0.05 mag.

Given these uncertainties, we continue to adopt the Hill et al. (1998) calibration, but we note that CTE effects render our distance moduli more uncertain than we have previously estimated. The modulus uncertainty adopted here is ± 0.09 mag. That makes Stetson's M92 results a 1.5 σ anomaly. Physically, the M92 results seem anomalous, since CTE correction should be intrinsically gray. Further investigation of the zero point for the Cepheid photometry database is required.

REFERENCES

Aaronson, M., Huchra, J., Mould, J., Schechter, P., & Tully, R. B. 1982, ApJ, 258, 64 (AHMST)
Aaronson, M., & Mould, J. 1986, ApJ, 303, 1
Aaronson, M., Mould, J., Huchra, J., Sullivan, W., Schommer, R., & Bothun, G. 1980, ApJ, 239, 12
Burstein, D., Davies, R., Dressler, A., Faber, S., Lynden-Bell, D., Terlevich, R., & Wegner, G. 1986, in Galaxy Distances and Deviations from Universal Expansion, ed. B. Madore & R. B. Tully (Dordrecht: Reidel), 123
Davis, M., Tonry, J., Huchra, J., & Latham, D. 1980, ApJ, 238, L113
Dekel, A., et al. 1999, ApJ, 522, 1
de Vaucouleurs, G. 1958, AJ, 63, 253
———. 1972, in IAU Symp. 44, External Galaxies and Quasistellar Objects, ed. D. Evans (Dordrecht: Reidel), 353
Faber, S., & Burstein, D. 1989, in Large Scale Motions in the Universe, ed. V. Rubin & G. Coyne (Princeton: Princeton Univ. Press), 115
Ferrarese, L., et al. 2000a, ApJ, 529, this issue
———. 2000b, ApJS, submitted
Freedman, W. 1999, in Particle Physics and the Universe, ed. L. Bergstrom, P. Carlson, & C. Frannson (Singapore: World Scientific), in press (preprint astro-ph/9905222)
Gibson, B., et al. 2000, ApJ, 529, this issue
Giovanelli, R., Haynes, M., Salzer, J., Wegner, G., da Costa, L., & Freudling, W. 1998, AJ, 116, 2632
Gonzaga, S., et al. 1999, BAAS, 30, 1298
Gonzales, A., & Faber, S. 1997, ApJ, 485, 80
Hamuy, M., Phillips, M., Suntzeff, N., Schommer, R., Maza, J., & Aviles, R. 1996, AJ, 112, 2398
Han, M. 1992, ApJ, 395, 75
Han, M., & Mould, J. 1990, ApJ, 360, 448
Heyer, I., et al. 1999, BAAS, 30, 1299
Hill, R., et al. 1998, ApJ, 496, 648
Holtzman, J. A., et al. 1995, PASP, 107, 1065
Kelson, D., et al. 2000, ApJ, 529, this issue
Kennicutt, R. C., Jr., Freedman, W. L., & Mould, J. R. 1995, AJ, 110, 1476
Kennicutt, R. C., Jr., et al. 1998, ApJ, 498, 181
Kogut, A., et al. 1993, ApJ, 419, 1
Lauer, T., & Postman, M. 1994, ApJ, 425, 418
Lynden-Bell, D., Faber, S., Burstein, D., Davies, R., Dressler, A., Terlevich, R., & Wegner, G. 1988, ApJ, 326, 19

Madore, B., & Freedman, W. 1991, PASP, 103, 933
Madore, B., et al. 1998, Nature, 395, 47
Marinoni, C., et al. 1998a, ApJ, 505, 484
Marinoni, C., Giuricin, G., Constantini, B., & Monaco, P. 1998b, in ASP Conf. Ser. 146, The Young Universe: Galaxy Formation and Evolution at Intermediate and High Redshift, ed. S. D'Odorico, A. Fontana, & E. Giallongo (San Francisco: ASP), 202
Peebles, P. J. E. 1976, ApJ, 205, 318
Phillips, M., Lira, P., Suntzeff, N., Schommer, R., Hamuy, M., & Maza, J. 1999, AJ, 118, 1766
Riess, A., Press, W., & Kirshner, R. 1995, ApJ, 445, L91
Rowan-Robinson, M. 1986, The Cosmological Distance Ladder: Distance and Time in the Universe (New York: Freeman)
Sakai, S., et al. 2000, ApJ, 529, this issue
Sandage, A. 1996, AJ, 111, 18
Scaramella, R., et al. 1989, Nature, 338, 562
Schechter, P. 1980, AJ, 85, 801
Schmidt, B., et al. 1994, ApJ, 432, 42
Shaya, E., Tully, R. B., & Pierce, M. 1992, ApJ, 391, 16
Shi, X., & Turner, M. 1998, ApJ, 493, 519
Silk, J. 1974, ApJ, 193, 525
Stetson, P. 1998, PASP, 110, 1448
Strauss, M., & Willick, J. 1995, Phys. Rep., 261, 271
Tammann, G. 1998, 8th Marcel Grossman Symp., ed. T. Piran (Singapore: World Scientific), in press.
Tanvir, N. 1999, ASP Conf. Ser. 167, Harmonizing Cosmic Distance Scales in a Post-Hipparcos Era, ed. D. Egret & A. Heck (San Francisco: ASP), 64
Tonry, J., Blakeslee, J., Ajhar, E., & Dressler, A. 1997, ApJ, 475, 399
Tonry, J., & Davis, M. 1981, ApJ, 246, 680
Tully, R. B., & Fisher, J. R. 1987, Atlas of Nearby Galaxies (Cambridge: Cambridge Univ. Press)
Westerlund, B. E. 1996, The Magellanic Clouds (Cambridge: Cambridge Univ. Press)
Whitmore, B., & Heyer, I. 1997, Instrument Science Rept. WFPC2 97-08 (Baltimore: STScI)
Wiggs, M., et al. 1999, BAAS, 30, 1298
Yahil, A., Tammann, G., & Sandage, A. 1977, ApJ, 217, 903
Zehavi, I., Riess, A., Kirshner, R., & Dekel, A. 1998, ApJ, 503, 483

ERRATUM

In the article "The *Hubble Space Telescope* Key Project on the Extragalactic Distance Scale. XXVIII. Combining the Constraints on the Hubble Constant" (ApJ, 529, 786 [2000]), by Jeremy R. Mould, John P. Huchra, Wendy L. Freedman, Robert C. Kennicutt, Jr., Laura Ferrarese, Holland C. Ford, Brad K. Gibson, John A. Graham, Shaun M. G. Hughes, Garth D. Illingworth, Daniel D. Kelson, Lucas M. Macri, Barry F. Madore, Shoko Sakai, Kim M. Sebo, Nancy A. Silbermann, and Peter B. Stetson, some sign errors need to be corrected.

1. In equation (A2) the minus signs should be plus signs. The correct version is

$$V_{\text{cosmic}} = V_H + V_{c,\text{LG}} + V_{\text{in,Virgo}} + V_{\text{in,GA}} + V_{\text{in,Shap}} + \cdots . \tag{A2}$$

2. In Table A1 the declination of the Great Attractor (GA) is $-44°$, and that of the Shapley supercluster is $-31°$, i.e., south declination, not north, as implied in the table.

The first error is the authors' and the second occurred in the publication process. In both cases the computer code was correct, and the errors are in the published representation. None of the results presented in the paper are therefore affected in any way.

The authors thank Dr. Jim Condon for pointing out the error in equation (A2).